the plant journal

SEB Society for Experimental Biology

The Plant Journal (2015) **84,** 1005–1020 doi: 10.1111/tpj.13060

Chloroplast lipid transfer processes in *Chlamydomonas reinhardtii* involving a TRIGALACTOSYLDIACYLGLYCEROL 2 (TGD2) orthologue

Jaruswan Warakanont[1,2], Chia-Hong Tsai[1,2,†], Elena J. S. Michel[1,‡], George R. Murphy III[3,§], Peter Y. Hsueh[3,¶], Rebecca L. Roston[3,], Barbara B. Sears[1,2] and Christoph Benning[2,3,*]**

[1]*Department of Plant Biology, Michigan State University, East Lansing, Michigan 48824, USA,*
[2]*MSU-DOE Plant Research Laboratory, Michigan State University, East Lansing, Michigan 48824, USA, and*
[3]*Department of Biochemistry and Molecular Biology, Michigan State University, East Lansing, Michigan 48824, USA*

Received 5 August 2015; revised 5 October 2015; accepted 16 October 2015; published online 23 October 2015.
*For correspondence (e-mail benning@msu.edu).
†Present address: Amyris Inc. 5885 Hollis St. Suite 100, Emeryville, CA 94608, USA.
‡Present address: Plant Biology Program, Cornell University, Ithaca, New York 14853, USA.
§Present address: Department of Biological Chemistry, University of Michigan, Ann Arbor, Michigan 48109, USA.
¶Present address: Cell and Molecular Biology Program, Michigan State University, East Lansing, Michigan 48824, USA.
**Present address: Department of Biochemistry, University of Nebraska-Lincoln, Lincoln, Nebraska 68588, USA.

SUMMARY

In plants, lipids of the photosynthetic membrane are synthesized by parallel pathways associated with the endoplasmic reticulum (ER) and the chloroplast envelope membranes. Lipids derived from the two pathways are distinguished by their acyl-constituents. Following this plant paradigm, the prevalent acyl composition of chloroplast lipids suggests that *Chlamydomonas reinhardtii* (Chlamydomonas) does not use the ER pathway; however, the Chlamydomonas genome encodes presumed plant orthologues of a chloroplast lipid transporter consisting of TGD (TRIGALACTOSYLDIACYLGLYCEROL) proteins that are required for ER-to-chloroplast lipid trafficking in plants. To resolve this conundrum, we identified a mutant of Chlamydomonas deleted in the *TGD2* gene and characterized the respective protein, CrTGD2. Notably, the viability of the mutant was reduced, showing the importance of CrTGD2. Galactoglycerolipid metabolism was altered in the *tgd2* mutant with monogalactosyldiacylglycerol (MGDG) synthase activity being strongly stimulated. We hypothesize this to be a result of phosphatidic acid accumulation in the chloroplast outer envelope membrane, the location of MGDG synthase in Chlamydomonas. Concomitantly, increased conversion of MGDG into triacylglycerol (TAG) was observed. This TAG accumulated in lipid droplets in the *tgd2* mutant under normal growth conditions. Labeling kinetics indicate that Chlamydomonas can import lipid precursors from the ER, a process that is impaired in the *tgd2* mutant.

Keywords: lipid metabolism, *Chlamydomonas reinhardtii*, chloroplast lipids, membranes, lipid transport.

INTRODUCTION

Microalgae play an important role as primary biomass producers in diverse ecosystems through their ability to efficiently convert solar into chemical energy. In fact, estimates based on radioactive bicarbonate labeling of seawater samples from the Atlantic Ocean suggest that marine algae account for nearly a quarter of total global carbon fixation (Jardillier *et al.*, 2010), which is in part a result of their high photosynthetic efficiency (Melis, 2009; Weyer *et al.*, 2010). In addition to their importance in natural ecosystems, microalgae have received special attention as biofuel feedstocks because of their rapid life cycle and their potential to accumulate high levels of biomass in limited space.

Chlamydomonas reinhardtii (Chlamydomonas) is a unicellular green alga that has served for many decades as an instructive model in studies of photosynthesis, flagella development and function, and more recently to explore the regulation of metabolism in response to different growth conditions. Chlamydomonas cells are haploid during vegetative growth and the Chlamydomonas genome often has a single copy of many plant orthologous genes, thereby facilitating genotype–phenotype relationship studies. Finally, the availability of multiple resources including a sequenced genome (Merchant *et al.*, 2007) facilitates research on this microalga.

Photosynthesis takes place in thylakoid membranes in bacterial cells or inside chloroplasts present in algae and plants. Photosynthetic membranes from the cyanobacteria, the presumed predecessor of chloroplasts, algae and plants analyzed to date contain four lipids: the two galactoglycerolipids mono- (MGDG) and digalactosyldiacylglycerol (DGDG), the sulfoglycerolipid sulfoquinovosyldiacylglycerol (SQDG), and the only phosphoglycerolipid phosphatidylglycerol (PtdGro) (Boudière *et al.*, 2014). With their different properties, each lipid class plays distinct roles in photosynthetic membranes. Therefore, these four lipids are present in a conserved ratio in order to maintain the structure and function of photosynthetic membranes (Boudière *et al.*, 2014).

Among these conserved lipids, the galactoglycerolipids MGDG and DGDG are the most abundant throughout Viridiplantae (Boudière *et al.*, 2014). In plants, the galactoglycerolipids are synthesized either through the eukaryotic or through the prokaryotic pathways (Roughan and Slack, 1982). In the case of the eukaryotic pathway, fatty acids synthesized in the chloroplast are exported, converted to acyl-CoAs and incorporated at the endoplasmic reticulum (ER) into membrane lipids, e.g. phosphatidic acid (PtdOH) or phosphatidylcholine (PtdCho). ER-assembled lipids then return to the chloroplast and are converted to diacylglycerol (DAG), which is then galactosylated in the two envelope membranes to form MGDG and subsequently DGDG. In contrast, the prokaryotic pathway in plants and algae occurs entirely in the chloroplast envelope membranes. Fatty acyl groups attached to acyl carrier proteins (ACPs) synthesized in the chloroplast are incorporated directly into lipid precursors to give rise to PtdOH, DAG and then galactoglycerolipids. In plants, the bulk of MGDG is synthesized in the inner envelope, whereas DGDG is synthesized at the outer envelope, requiring an exchange of lipids between the two envelope membranes (Benning, 2009).

In plants, lipids derived from either pathway can be distinguished by the number of carbons at the *sn–2* position of the glyceryl backbone: 16–carbon fatty acids (C16) for the prokaryotic and 18–carbon fatty acids (C18) for the eukaryotic pathway-derived lipids, respectively (Heinz and Roughan, 1983). This is thought to result from the substrate specificity of lyso-PtdOH acyltransferases located in the chloroplast that prefer C16, whereas those at the ER prefer C18 (Roughan and Slack, 1982; Frentzen *et al.*, 1983; Kunst *et al.*, 1988; Kim *et al.*, 2005). Because Chlamydomonas has exclusively C16 fatty acids at the *sn*–2 position of its galactoglycerolipids, it is thought not to use the eukaryotic pathway for galactoglycerolipid synthesis, and therefore should not require ER-to-chloroplast lipid trafficking (Giroud and Eichenberger, 1988); however, this conclusion is based on the untested assumption that the lyso-PtdOH acyltransferases at the ER and the chloroplast membranes in plants and Chlamydomonas have the same distinct substrate specificity.

In Arabidopsis, the ER-to-chloroplast lipid trafficking of the eukaryotic pathway is mediated through TRIGALACTOSYLDIACYLGLYCEROL (TGD1, -2, -3 and -4) proteins (Xu *et al.*, 2003, 2008; Awai *et al.*, 2006; Lu *et al.*, 2007) and a recently discovered TGD5 protein (Fan *et al.*, 2015). Mutations in any of the respective Arabidopsis genes cause a secondary phenotype resulting in the accumulation of oligogalactolipids, e.g. trigalactosyldiacylglycerol (TGDG), after which the mutants were named. These oligogalactolipids are synthesized by the activation of a galactolipid: galactolipid galactosyltransferase encoded by *SENSITIVE TO FREEZING 2* (*SFR2*), a gene absent from Chlamydomonas, which, therefore, presumably does not synthesize oligogalactolipids. In Arabidopsis, TGD1, -2 and -3 form an ATP-binding cassette (ABC) transporter complex in the inner envelope membrane of the chloroplast, and function as a permease, a substrate binding protein and an ATPase, respectively (Benning, 2009; Roston *et al.*, 2012). TGD4 is localized in the outer envelope membrane of the chloroplast as a homodimer (Wang *et al.*, 2012). It has been suggested that TGD4 transports the ER lipid precursor from the ER to the TGD1, -2, -3 complex (Benning, 2009; Hurlock *et al.*, 2014), and that TGD5 links this complex to TGD4 (Fan *et al.*, 2015). The TGD1, -2, -3 complex then transfers the ER lipid precursor to the inner envelope membrane of the chloroplast. It should be noted that the exact nature of the transported lipid species for the TGD1, -2, -3 complex or TGD4 is not known at this time.

Bacterial orthologues of TGD proteins have been suggested to be involved in resistance to organic solvents or toxic chemicals. In *Pseudomonas putida*, TtgA, -B and -C (toluene tolerance genes) and SrpA, -B and -C (solvent-resistant pump) have been proposed to act as toluene efflux pumps, although their direct biochemical function has yet to be demonstrated (Kieboom *et al.*, 1998a,b; Kim *et al.*, 1998; Ramos *et al.*, 1998). Loss of function of these proteins leads to toluene sensitivity. In *Escherichia coli*, MlaD, -E and -F proteins are proposed to function in maintaining an asymmetric lipid distribution in the outer membrane (Malinverni and Silhavy, 2009). The loss of function of any of these proteins results in increased outer membrane permeability, possibly through an inability to remodel the outer membrane lipid composition in response to chemical stress. The implication is that the bacterial orthologues of the plant TGD proteins transport lipids between the cell membrane and the outer membrane to allow remodeling in response to chemical insults.

The genome of Chlamydomonas harbors genes encoding putative TGD1, -2 and -3 orthologues (Merchant *et al.*,

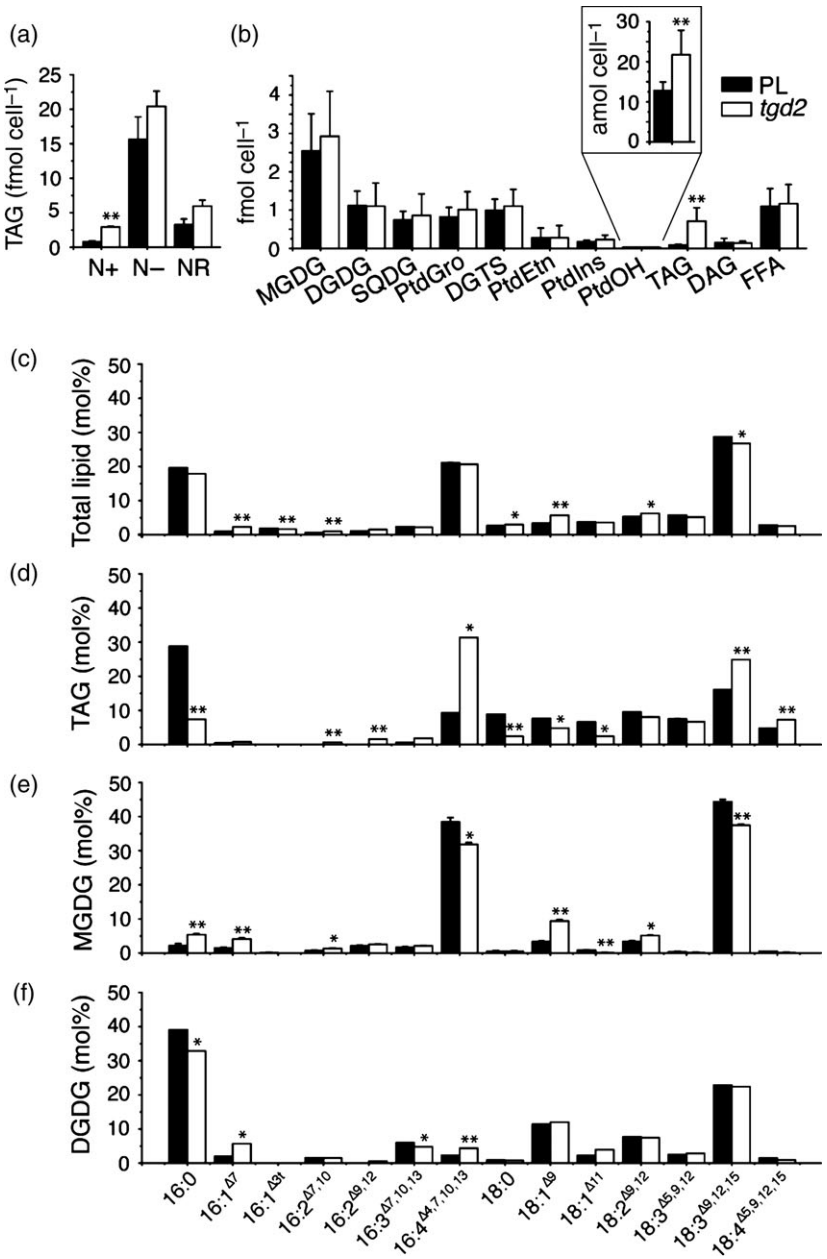

Figure 1. Lipid phenotypes of the Chlamydomonas *tgd2* mutant.

(a) Triacylglycerol (TAG) concentration in fmol cell^{-1} of parental line (dw15.1) PL (solid bars) and *tgd2* (open bars) grown in N–replete medium (N+) until mid-log phase, followed by 48 h of N deprivation (N–), followed by 24 h of N–resupply (NR).

(b) Cellular concentration of lipids of the PL and *tgd2* during mid-log phase grown in N–replete medium in order of presentation: monogalactosyldiacylglycerol, MGDG; digalactosyldiacylglycerol, DGDG; sulfoquinovosyldiacylglycerol, SQDG; phosphatidylglycerol, PtdGro; digalactosyl-*N,N,N*-trimethylhomoserine; DGTS; phosphatidylethanolamine, PtdEtn; phosphatidylinositol, PtdIns; phosphatidic acid, PtdOH; triacylglycerol, TAG; diacylglycerol, DAG; and free fatty acids, FFA.

(c) Acyl group profile of total lipids of the PL and *tgd2* during mid-log phase grown in N–replete medium. Standard nomenclature for fatty acids is used, and is indicated below the *x*–axis in (f): number of carbons:number of double bonds, with position of double bonds indicated counting from the carboxyl end.

(d) Acyl group profile of TAG of the PL and *tgd2* during mid-log phase grown in N–replete medium.

(e) Acyl group profile of MGDG of the PL and *tgd2* during mid-log phase grown in N–replete medium.

(f) Acyl group profile of DGDG of the PL and *tgd2* during mid-log phase grown in N–replete medium. In all cases, three biological replicates were averaged and standard deviations are shown. Differences in means of PL and *tgd2* were compared with a paired-sample Student's *t*–test (*$P \leq 0.05$; **$P \leq 0.01$).

2007). This raises two possibilities: (i) if Chlamydomonas does not require the import of lipids from the ER for thylakoid lipid assembly, as suggested by the molecular species composition of its thylakoid lipids, these proteins may be primarily involved in transferring lipids between the two envelope membranes, similar to the case in bacteria; (ii) alternatively, these proteins are involved in lipid trafficking from the ER to the chloroplast, in which case the plant paradigm for distinguishing thylakoid lipid species derived from the ER versus the chloroplast species does not apply to Chlamydomonas. To test these possibilities, we identified and studied a Chlamydomonas mutant deleted in *TGD2*.

RESULTS

The *tgd2* mutant accumulates triacylglycerol enriched in MGDG acyl groups

Triacylglycerols (TAGs) typically accumulate to high levels in Chlamydomonas only following nutrient deprivation, and are degraded following refeeding. The *tgd2* mutant was generated by insertional mutagenesis and identified during a screen for mutants delayed in TAG degradation following nitrogen (N) deprivation and refeeding (Tsai *et al.*, 2014). When TAG levels were monitored during N–replete, N–deprived and N–resupplied growth conditions, the *tgd2* mutant showed elevated levels under all

conditions tested (Figure 1a). Therefore, we focused the subsequent analyses on cells grown in N–replete medium. When the steady-state levels of all glycerolipids and free fatty acids (FFAs) were analyzed during N–replete growth, only TAG and PtdOH were increased with statistical significance in *tgd2* compared with the parental line (PL; Figure 1b). The central lipid intermediate PtdOH was the least abundant lipid included in the analyses, and was identified based on its relative co-chromatography with standards (Figure S1a) and its distinct acyl composition. Whereas the ratios of different acyl groups in the total lipid fraction did not obviously change (Figure 1c), the TAG fraction of *tgd2* was enriched in $16{:}4^{\Delta4,7,10,13}$ and $18{:}3^{\Delta9,12,15}$ acyl groups (number of carbons:number of double bonds with $^{\Delta Number}$, indicating the position of the double bond counted from the carboxyl end), with a concomitant reduction in the 16:0 acyl groups (Figure 1d) normally found in TAG synthesized following nutrient deprivation. These highly unsaturated acyl groups are typically found only in MGDG (Figure 1e), and their abundance in TAG of *tgd2* suggests that its DAG moiety or its acyl groups are derived from MGDG.

Subtle changes in MGDG and DGDG molecular species were also notable. In MGDG of *tgd2*, higher levels of 16:0, 16:1 and 18:1, and lower levels of $16{:}4^{\Delta4,7,10,13}$ and $18{:}3^{\Delta9,12,15}$, were observed (Figure 1e). In the case of DGDG of *tgd2*, the levels of 16:0 and 16:3 were reduced, whereas those of 16:1 and 16:4 were increased (Figure 1f). We specifically tested whether the Chlamydomonas *tgd2* mutant accumulates TGDG, as observed for Arabidopsis *tgd* mutants; however, none of the Chlamydomonas samples showed TGDG detectable by thin-layer chromatography (Figure S1b), consistent with the absence of an SFR2-like activity from Chlamydomonas.

Cultures of *tgd2* show early senescence

During routine maintenance of long-term cultures on agar-solidified medium, we observed that the *tgd2* mutant had a shorter culture lifespan than the PL. Subsequently, viability assays were carried out to further investigate this phenotype. Liquid cultures of PL, *tgd2* and *TGD2 tgd2* cells (a complemented line expressing *TGD2* in the *tgd2* mutant background, see below) were inoculated at 0.5×10^6 cells ml^{-1}. Cultures were examined after 3, 7, 14, 21 and 28 days. After 21 days, the *tgd2* culture began to turn yellow, which was even more obvious on day 28 (Figure 2a). This observation correlated with a continuously increasing fraction of dead cells over time observed in the *tgd2* culture using live cell stains (methylene blue and phenosafranin; Figure S2a). The *tgd2* culture accumulated more TAG throughout the culturing time (Figure 2b), and at day 3 substantial levels of MGDG-derived acyl groups were detected in the TAG fraction (Figure S2b). It seems likely that initially TAG is derived from the turnover of fully

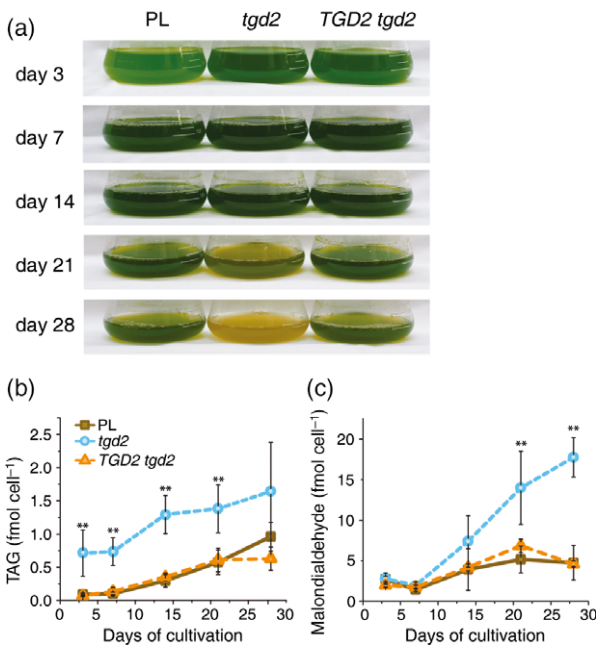

Figure 2. Viability assay for the parental line (PL; dw15.1), *tgd2* and complemented line *TGD2 tgd2* grown in N–replete medium.
(a) Images of cultures of PL, *tgd2* and *TGD2 tgd2* at days 3, 7, 14, 21 and 28 of cultivation. The culture was inoculated at 0.5×10^6 cells ml^{-1} on day 1.
(b) Cellular concentration of triacylglycerol (TAG, fmol/cell) in the PL, *tgd2* and *TGD2 tgd2* at days 3, 7, 14, 21 and 28 of cultivation.
(c) Cellular concentration of malondialdehyde (fmol/cell) of the PL, *tgd2* and *TGD2 tgd2* at day 3, 7, 14, 21 and 28. In all cases error bars indicate standard deviations based on three replicates. Analyses of variance was performed with ORIGIN PRO 8.0 (**$P \leq 0.01$).

desaturated MGDG, peaking at day 3, whereas later during prolonged culturing, as nutrients are depleted, *de novo* TAG synthesis is induced. This is indicated by a steady increase of 16:0 and $18{:}1^{\Delta9}$ acyl groups characteristic of *de novo* synthesized TAG. The prolonged culturing of *tgd2* also led to an accumulation of high levels of malondialdehyde, which is a product of the reaction between polyunsaturated acyl groups and reactive oxygen species (ROS; Figure 2c). As cells die, ROS typically accumulate, consistent with the observed decrease in the viability of the *tgd2* mutant.

Changes in the ultrastructure of *tgd2* cells

The original *tgd2* mutant was isolated in the cell wall mutant background dw15.1; however, strains with cell walls (cw^+) are more amenable to ultra-thin sectioning for transmission electron microscopy (TEM) than are cw^- lines, such as dw15.1. Hence, we moved the *tgd2* mutation into a cw^+ line, by crossing it with wild-type strain CC-198. For the TEM studies, the *tgd2* mutant was compared with CC-198 to determine ultrastructural changes caused by the *tgd2* mutation at mid-log, stationary and late stationary phases. In contrast to CC-198 (Figure 3a–c), which

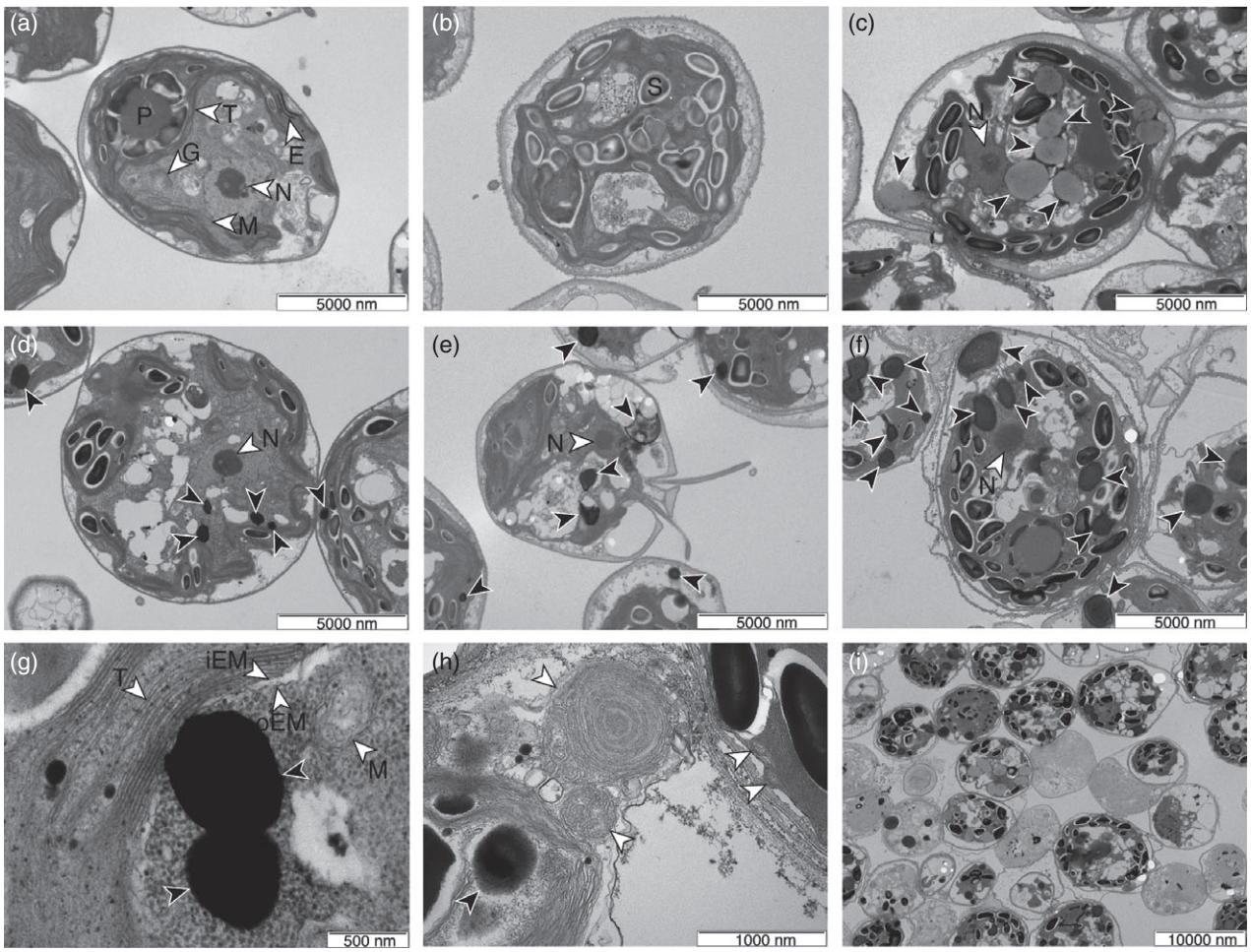

Figure 3. Ultrastructural changes in the *tgd2* mutant.
Electron micrographs of the wild-type cw$^+$ strain (CC-198) and *tgd2* grown in N–replete medium are shown during mid-log phase (day 3), stationery phase (day 10) and late stationary phase (day 17). Black and white arrows indicate lipid droplets and other organelles, respectively. Scale bars represent size, as indicated.
(a) Cells of CC-198 during mid-log growth with subcellular structures abbreviated: eyespot, E; Golgi apparatus, G; mitochondria, M; nucleus, N; pyrenoid, P; and thylakoid membrane, T.
(b) Cells of CC-198 during stationery phase with starch granules (S).
(c) Cells of CC-198 during late stationary phase.
(d) Cells of *tgd2* during mid-log phase.
(e) Cells of *tgd2* during stationary phase.
(f) Cells of *tgd2* during late stationary phase.
(g) Representative *tgd2* cell during mid-log phase showing the thylakoid membrane (T), the chloroplast inner envelope membrane (iEM), the chloroplast outer envelope membrane (oEM), mitochondria (M) and electron-dense lipid droplets (black arrows).
(h) Representative *tgd2* cell during late stationary phase showing compromised membrane structures (white arrows).
(i) Population of *tgd2* cells during late stationary phase showing dead and living cells.

contained lipid droplets during the late stationary phase (black arrows), *tgd2* showed lipid droplets at every time point (Figure 3d–f, black arrows). The *tgd2* mutant had more lipid droplets, which grew larger in size over time. These lipid droplets were observed in the cytoplasm of *tgd2* also harboring mitochondria, and were often adjacent to the chloroplast outer envelope membrane (Figure 3g). In addition, lipid droplets from the *tgd2* mutant stained darker (Figure 3d–g compared with 3c, black arrows), which is consistent with a higher desaturation level of TAGs as osmium tetroxide stains unsaturated lipids more intensely. During the late stationary phase at day 17, membranes of *tgd2* became disorganized (Figure 3h, white arrows) compared with the PL and earlier stages of *tgd2* (Figure S3). About half of the population appeared to be dead ghost cells, lighter in color and with less distinct internal structures (Figure 3i). Although a cw$^+$ complemented line was not available for this experiment, these ultrastructural changes corroborate observations made on the *tgd2* mutant and complemented lines in the dw15.1

background described above, and are likely to result from the ablation of the *TGD2* gene.

Molecular and genetic analyses of the *tgd2* mutant locus

The *tgd2* mutant was generated by the random genomic insertion of a plasmid carrying the Hygromycin B resistant gene (*Aph7*). Southern-blot analyses of genomic DNA of *tgd2* cut with *Bam*HI, and using a probe covering a region of *Aph7* that does not contain the *Bam*HI restriction site, indicated the presence of a single insertion (Figure S4). As a first step to identify the mutant locus, a genetic analysis was carried out to determine the linkage of the primary lipid phenotype and the Hygromycin B resistance marker. For this purpose, as already mentioned above, CC-198 was crossed with *tgd2* in the dw15.1 background. The progenies of this cross were tested for TAG content, TAG acyl profile and sensitivity to Hygromycin B. Without exception, all Hygromycin B-resistant progenies tested (11 resistant and 12 susceptible progenies from six zygotes) showed high TAG levels and TAGs with highly unsaturated acyl groups (Figure S5a,b). This result suggested close linkage of the Hygromycin B-resistant marker and the mutation that caused the TAG phenotype of the *tgd2* mutant.

As PCR-based methods were not successful in identifying DNA sequences flanking the Hygromycin B marker, whole-genome resequencing was used to determine the location of the mutation responsible for the primary phenotype in the genome of the *tgd2* mutant. Towards this end, genomic DNA of the *tgd2* mutant was subjected to Illumina-HiSeq paired-end sequencing. The reads were *de novo* assembled with VELVET 1.2.07 (Zerbino and Birney, 2008) using a *k*-mer length of 21. Contigs containing *Aph*7 were searched against the Chlamydomonas reference genome (v5.3) to identify flanking sequences, revealing a possible insertion site in chromosome 16. When the respective section of the reference genome of chromosome 16 was used as a template for the assembled contigs from the *tgd2* genome, a 31–kb deletion in chromosome 16 of *tgd2* became apparent. This deletion, which was confirmed by PCR probing, affected six genes either fully or partially, as shown in Figure S6a.

We introduced into *tgd2* genomic DNA fragments containing each affected gene (from approximately 1 kb 5′ of the start codon to about 0.5 kb 3′ of the stop codon) derived from a bacterial artificial chromosome covering the region. Each genomic DNA fragment was co-introduced into *tgd2* along with a linearized Paromomycin resistance gene (*Aph8*), which was under selection. Of the six genes disrupted or missing from the *tgd2* genome, only the introduction of *CrTGD2* was able to restore TAG content, TAG acyl group profile, cell viability and PtdOH content close to PL levels (Figure S6). Therefore, the deletion of *TGD2* is the cause of at least four phenotypes of the *tgd2* mutant discussed. Because the phenotype of complemented line C3 was nearly fully restored to that of the PL (Figure S6b,c), this line was included in all subsequent analyses, except where indicated otherwise, and is designated *TGD2 tgd2*.

***CrTGD2* is a presumed orthologue of AtTGD2**

The translated sequence of the Chlamydomonas *CrTGD2* gene has 40% amino acid identity with the Arabidopsis protein AtTGD2. Both are similar to substrate binding protein components of bacterial ABC transporters (Casali and Riley, 2007). Both also contain a mammalian cell entry (MCE) domain (Figure S7), which, in the respective *Mycobacterium tuberculosis* protein for which this domain was named, is required for pathogenesis. In addition phylogenetic analyses of the MCE domain of predicted CrTGD2 orthologues across plants, green algae and bacteria revealed that CrTGD2 falls into the same clade as the respective plant proteins, and is divergent from bacterial orthologues (for the alignment, see Figure S8 and Appendix S1). Using TMHMM (Krogh *et al.*, 2001), CrTGD2 is predicted to contain one transmembrane domain (Figure S7), similar to the Arabidopsis orthologue AtTGD2 (Awai *et al.*, 2006). Based on these similarities, we hypothesized that CrTGD2 may have similar functions as AtTGD2 and, hence, those two proteins may be true orthologues. To more directly test their functional equivalence, we introduced: (i) codon-optimized Arabidopsis TGD2 into the Chlamydomonas *tgd2* mutant; and (ii) Chlamydomonas TGD2 into the Arabidopsis *tgd2–1* mutant. Despite the presence of the recombinant proteins, however, lipid phenotypes were not restored (Figures S9 and S10). Thus, the two TGD2 proteins seem to be sufficiently divergent to not substitute for each other in a heterologous protein complex.

Altered galactoglycerolipid labeling and impaired ER-to-plastid lipid trafficking in *tgd2*

Pulse-chase analyses provides a proven *in vivo* method to examine general substrate–product relationships in metabolic pathways, and lipid trafficking in plants in particular, and it was used in the original analyses of the *tgd1–1* mutant of Arabidopsis, (e.g. Xu *et al.*, 2003). Here, we carried out pulse-chase labeling experiments with [^{14}C]acetate using mid-log phase cultures of the PL, *tgd2* and *TGD2 tgd2*. The cells were incubated in the presence of labeled substrate until 20–40% incorporation of label was observed before the labeled medium was replaced for the chase. Total lipids were extracted at different times during the chase phase, and individual lipids were separated by thin-layer chromatography followed by liquid scintillation counting to determine the fraction of incorporation of radiolabel into all lipids analyzed. Multiple individual repetitions of this experiment were carried out and all of these replicates showed similar trends, but the absolute values differed, making it difficult to average results from the

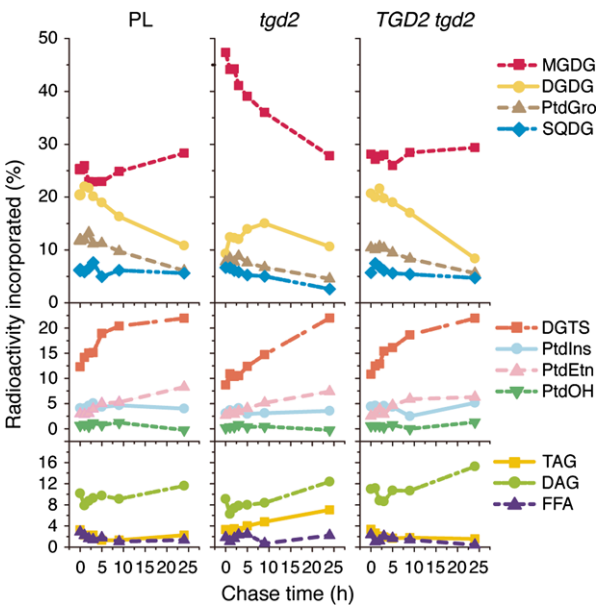

Figure 4. [^{14}C]Acetate pulse-chase labeling of parental line (PL; dw15.1), *tgd2* mutant and *TGD2 tgd2* complemented line.
Cells were labeled with [^{14}C]acetate until 20–40% of the label was incorporated (pulse). The chase shown here beginning at time 0 (h) was initiated by changing to unlabeled medium. The fraction of label found in each lipid (%) relative to the total label incorporated in the lipid fraction is shown during the 24–h chase time course. Abbreviations of the lipids are as defined in the legend to Figure 1. Results from one representative experiment of four are shown.

different experiments. Therefore, a representative experiment is shown in Figure 4.

The most noticeable differences in labeling between the different cell lines were observed for MGDG and DGDG. MGDG in *tgd2* was labeled to much higher levels, with a subsequent rapid decrease in label during the chase phase (Figure 4, top panels). In contrast, MGDG labeling in PL and in the *TGD2 tgd2* line was lower, and less of a decrease in label was observed during the chase. As the bulk steady-state levels of MGDG in *tgd2* did not significantly change compared with the PL (Figure 1b), the result suggests that MGDG was more rapidly synthesized and metabolized in *tgd2*. As DGDG is derived from MGDG, one would expect that its labeling would follow that of MGDG, at least in the initial chase phase (within the first 5 h), and that label would appear to move from MGDG to DGDG, as was the case for the PL and *TGD2 tgd2* during the first 5 h of the chase. DGDG labeling was severely delayed and not as high in *tgd2* (Figure 4, top panels), however, suggesting a disruption in the conversion of MGDG to DGDG in *tgd2* or the activation of pathways competing for MGDG as a substrate.

The detailed shape of the time course for MGDG labeling was also different in the mutant. In the PL and *TGD2 tgd2* lines the MGDG labeling time course showed a 'dip' and rebound during the first 5 h of the initial stage of the chase, but in the *tgd2* mutant, MGDG labeling declined steadily (Figure 4, top panel). This result was not a chance observation of this particular experiment, because independent repeats showed this phenomenon reproducibly (Figure S11). The equivalent experiment with wild-type Arabidopsis leaves shows a comparable MGDG labeling time course, which is interpreted as an initial rapid labeling of MGDG by the chloroplast pathway, followed by label dilution during the initial chase phase decreasing the label, followed by a gradual increase in the labeling of MGDG over time as lipids move back from the ER as part of the ER pathway of galactoglycerolipid biosynthesis (Xu *et al.*, 2003). In the Arabidopsis *tgd1–1* mutant MGDG labeling is also very high and steadily declines during the chase phase, interpreted as a reduction in lipid species returning from the ER to the chloroplast. The observation of the typical 'dip' in MGDG labeling in the Chlamydomonas PL is currently the most direct indicator for ER-to-chloroplast lipid trafficking in this alga. The lack of the 'dip' in the *tgd2* mutant suggests that TGD2 is involved in this process.

Altered labeling of non-galactoglycerolipids in *tgd2*

In addition to the differences in MGDG and DGDG labeling, the labeling time course of the betaine lipid diacylglyceryltrimethylhomoserine (DGTS) and PtdGro also showed changes in the *tgd2* mutant. In contrast to the PL, DGTS labeling during the chase in *tgd2* started at a lower level and continued to increase without leveling off (Figure 4, middle panels). This result would be consistent with a decreased rate of precursor conversion into DGTS in the *tgd2* mutant. Less label was also found in PtdGro in *tgd2* (Figure 4, top panels), although the shape of the labeling time course looked similar to that of the PL and the *TGD2 tgd2* complemented line. It should be noted that DGTS and PtdGro steady-state levels were not altered in the mutant (Figure 1b). Therefore the relative rate of synthesis of these two lipids was decreased (or the turnover was increased) compared with that of MGDG in *tgd2*.

Although incorporation of label into the TAG fraction in the PL and the complemented line *TGD2 tgd2* was minimal, label in TAG of the *tgd2* mutant steadily increased during the chase phase, in parallel with a decrease of label in MGDG (Figure 4, lower panel). Given also the observation that MGDG-specific acyl groups were found in TAG under steady-state conditions in *tgd2* (Figure 1a,b,d,e), the labeling result was consistent with a conversion of mature MGDG to TAG in the *tgd2* mutant. The labeling of other lipids did not show much difference in the *tgd2* mutant (Figure 4).

Biosynthesis of MGDG is increased in the *tgd2* mutant

The increase in acetate labeling of MGDG prompted us to investigate MGDG synthesis directly by using a more

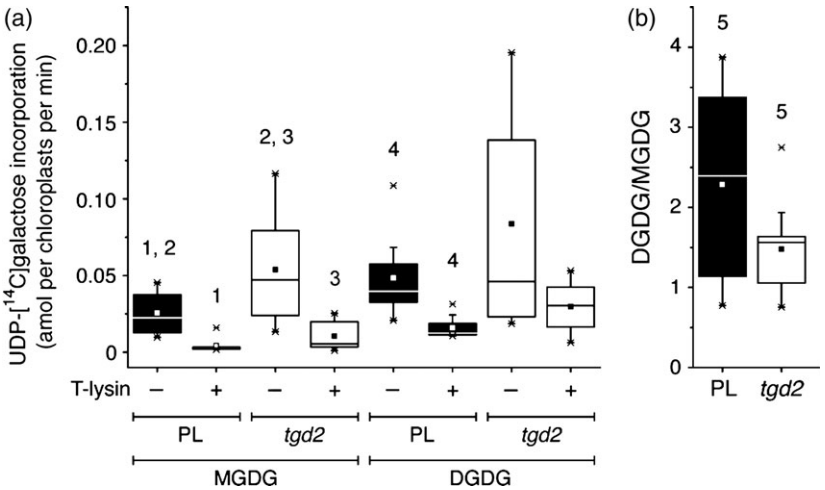

Figure 5. Galactoglycerolipid synthesis of parental line (PL; dw15.1) and *tgd2* chloroplasts.
(a) Incorporation of UDP-[^{14}C]galactose into monogalactosyldiacylglycerol (MGDG) and digalactosyldiacylglycerol (DGDG) of PL and *tgd2* chloroplasts. All samples were either not treated with protease (–) or treated (+) with Thermolysin (T–lysin), as indicated.
(b) Ratio of labeled DGDG/labeled MGDG from non-protease treated chloroplasts for the PL and the *tgd2* mutant. In each case nine replicates from different experiments were statistically analyzed for each treatment, and the results displayed as box plots (solid for PL, open for *tgd2*). A central square within each box plot represents the mean; the line represents the median. *Extreme values. Statistical tests of different means were performed using a paired-sample Student's *t*–test ($P \leq 0.05$). The following pairs indicated by numbers were significantly different: 1, MGDG PL (–) was significantly higher than MGDG PL (+); 2, MGDG PL (–) was significantly lower than MGDG *tgd2* (–); 3, MGDG *tgd2* (–) was significantly higher than MGDG *tgd2* (+); 4, DGDG PL (–) was significantly higher than DGDG PL (+). 5, DGDG/MGDG PL was significantly higher than DGDG/MGDG *tgd2*.

specific substrate, UDP-galactose. Intact chloroplasts from PL and *tgd2* were fed with 300 mCi mmol^{-1} UDP-[^{14}C]-galactose. Total lipids were extracted, and incorporation of labeled galactose into MGDG and DGDG was monitored and normalized based on an equal number of chloroplasts. We observed higher levels of labeled MGDG and DGDG in chloroplasts from *tgd2* than from the PL (Figure 5a), consistent with a higher galactolipid synthesis activity in the *tgd2* mutant. It is important to note that MGDG is synthesized by the addition of one galactose from UDP-galactose to DAG, and that DGDG is synthesized by the transfer of one galactose from UDP-galactose to MGDG. Thus, in the case of DGDG, four different molecular species can be obtained during this experiment, depending on whether only the distal or the proximal galactose, or both, or none of the galactoses are labeled. This makes it challenging to directly determine the MGDG–DGDG precursor product relationship. In order to compare rates of conversion of MGDG to DGDG, however, ratios of labeled DGDG/labeled MGDG were calculated. This ratio is significantly lower in *tgd2* (Figure 5b), which indicates a lower rate of conversion of MGDG to DGDG in *tgd2*.

In Arabidopsis, MGDG synthases can be localized in either of the two chloroplast envelope membranes (Awai *et al.*, 2001), but the bulk of MGDG synthesis involves MGD1 at the inner envelope membrane (Jarvis *et al.*, 2000). To test whether the observed MGDG synthase activity of isolated chloroplasts might be associated with the outer envelope membrane in Chlamydomonas, we treated the chloroplasts with Thermolysin, a large protease that cannot penetrate the outer envelope membrane (see also below). As shown in Figure 5a, MGDG and DGDG syntheses were sensitive to Thermolysin, suggesting that both the MGDG and the DGDG synthases are located in the outer envelope membrane in Chlamydomonas.

CrTGD2 is present in the inner chloroplast envelope membrane

Based on amino acid sequence analyses with different online prediction tools, including PredAlgo (Tardif *et al.*, 2012), the location of CrTGD2 was initially ambiguous, but likely in the chloroplast. Fractions containing chloroplasts, mitochondria and microsomal membranes were isolated from whole-cell lysates and CrTGD2 was detected using immunoblotting with antiserum raised against the recombinant protein. Antisera against marker proteins for each cell compartment were also tested. Whole-cell lysate of the *tgd2* mutant lacking CrTGD2 was used as a negative control to confirm the presence of the CrTGD2 signal in the PL extracts. As shown in Figure 6a, each subfraction was enriched with its respective marker protein, whereas CrTGD2 was clearly detected in the chloroplast fraction and whole-cell lysate. This suggests that CrTGD2 is localized in the chloroplast.

Because CrTGD2 was predicted to contain one transmembrane domain (Figure S7), a protease protection assay was carried out to determine the possible insertion of CrTGD2 into one of the chloroplast envelope

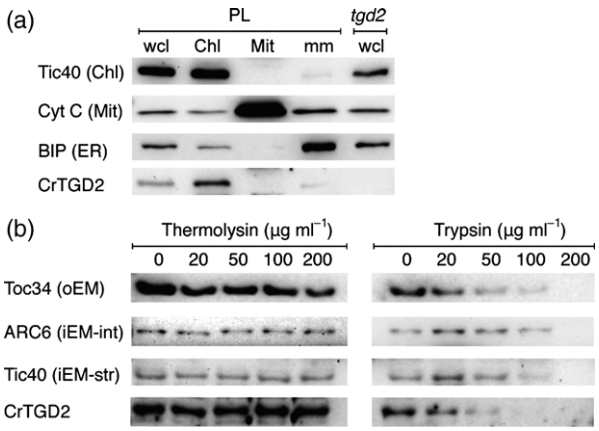

Figure 6. Localization of CrTGD2.
(a) Subcellular fractions of the parental line (PL; dw15.1) were compared with whole cell lysates of *tgd2*. Fractions of the PL were as follows: whole-cell lysate, wcl; chloroplasts, Chl; mitochondria, Mit; and microsomal membrane, mm. A Western blot is shown. Total protein of each fraction was used to detect: Tic40, a chloroplast marker (Chl); cytochrome *c* (Cyt C); a mitochondrial marker (Mit); BIP, an endoplasmic reticulum (ER) marker; and CrTGD2, using the respective antisera.
(b) Protease treatment of PL chloroplasts to determine the envelope membrane association of TGD2. Chloroplasts were treated with various concentrations of Thermolysin or Trypsin, as indicated. A Western blot is shown detecting Toc34, a chloroplast outer envelope membrane (oEM) marker, ARC6, a chloroplast inner envelope membrane marker facing the intermembrane space (iEM-int), Tic40, a chloroplast inner envelope membrane marker facing the stroma (iEM-str), and CrTGD2.

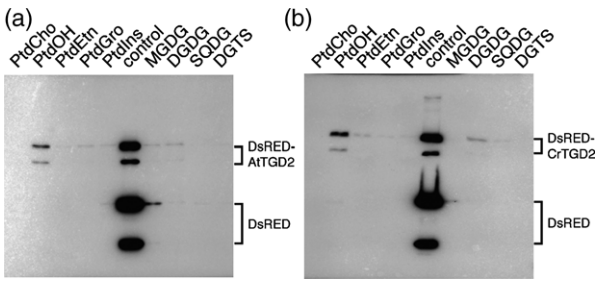

Figure 7. Lipid binding assay.
Liposomes made from different lipids, as indicated (see the legend to Figure 1 for lipid abbreviations), were incubated with DsRED-TGD2 recombinant proteins from Arabidopsis (a) or Chlamydomonas (b). Proteins associated with the liposomes were detected by Western blotting using a His-tag antibody. Each reaction contained DsRED protein as an internal negative control. A control lane containing 10% of the proteins without liposomes used in each assay is shown in the middle of each blot.

membranes. This assay takes advantage of the size difference between Thermolysin and Trypsin (Cline *et al.*, 1984). In general, Thermolysin is too big to penetrate the outer envelope membrane of the chloroplast. In contrast, Trypsin is sufficiently small to gain access to the intermembrane space and proteins in the inner envelope membrane. Different concentrations of either Thermolysin or Trypsin were used to treat isolated intact chloroplasts of the PL. Antisera against three markers for specific compartments were: anti-Toc34, detecting an outer envelope membrane protein; anti-ARC6, detecting an inner envelope membrane protein facing the intermembrane space; and anti-Tic40, detecting an inner envelope membrane protein facing the stroma. As a result of Thermolysin treatment at increasing concentrations, Toc34 decreased in abundance, as predicted for an outer envelope membrane protein, but the other markers and CrTGD2 did not (Figure 6b, left panel). Following treatment with Trypsin, all proteins were susceptible at increasing concentrations of the protease (Figure 6b, right panel). This result suggests that CrTGD2 is localized in the inner envelope membrane, as was previously observed for the AtTGD2 orthologue (Awai *et al.*, 2006).

CrTGD2 binds PtdOH *in vitro*

The Arabidopsis orthologue AtTGD2 binds PtdOH *in vitro* (Awai *et al.*, 2006; Lu and Benning, 2009). Therefore, a liposome binding assay was used to test for lipid binding by CrTGD2. As performed for AtTDG2, a recombinant CrTGD2 protein truncated from the N terminus to just beyond the membrane-spanning domain was fused to the C terminus of DsRED to improve solubility (Lu and Benning, 2009), and was produced in *E. coli*. This fusion protein also contained a His-tag at its C terminus and was designated DsRED-CrTGD2-His-tag. In parallel, DsRED-AtTGD2-His-tag was used as a positive control. As an internal negative control, DsRED by itself, which does not bind lipids, was included with the samples. Both AtTGD2 and CrTGD2 showed the strongest binding to PtdOH of all lipids tested (Figure 7a,b). The double band is the result of an internal autocatalytic cleavage of DsRED, as previously reported (Gross *et al.*, 2000).

DISCUSSION

Lipid metabolism of Chlamydomonas was thought to differ from that of Arabidopsis in at least three aspects: (i) Chlamydomonas does not synthesize PtdCho; (ii) Chlamydomonas has the betaine lipid DGTS; and (iii) Chlamydomonas is not thought to use the ER pathway for precursors of thylakoid lipid assembly (Giroud and Eichenberger, 1988). In fact, because the lipid precursor transported from the ER to the chloroplast is still unknown (Hurlock *et al.*, 2014), but might involve PtdCho, these three differences could be related. The genome of Chlamydomonas encodes TGD1, 2, and 3 proteins, however, which have been shown to be involved in lipid trafficking from the ER to the chloroplasts in Arabidopsis (Benning, 2009; Hurlock *et al.*, 2014). Thus, if Chlamydomonas were truly lacking ER-to-plastid lipid transport, the presence of these proteins in Chlamydomonas presents an interesting conundrum.

The analyses of the *tgd* mutants of Arabidopsis is complicated by the fact that the loss of function of *TGD* genes

is embryo-lethal, and that in the available leaky mutants a galactoglycerolipid-synthesizing enzyme, SFR2, is induced. Its activity leads to the formation of di- and higher order oligogalactoglycerolipids from MGDG. Therefore, the absence of SFR2 activity from Chlamydomonas allows us to reevaluate more directly the function of TGD proteins in the biosynthesis of the thylakoid lipids MGDG and DGDG in this organism, without having to consider the competing SFR2-based pathway present in Arabidopsis. Thus, studying the role of TGD2 in Chlamydomonas with a loss-of-function *tgd2* mutant that is not lethal, but has a rapid senescence phenotype, provides a unique opportunity to more fully understand the role(s) of TGD proteins in the chloroplast envelope membranes. Moreover, only single genes for MGDG and DGDG synthases, respectively, are present in the Chlamydomonas genome, further simplifying the analyses of its galactoglycerolipid metabolism. One caveat is that we do not yet know the exact location of the two galactoglycerolipid synthases in Chlamydomonas, but our analyses, based on the sensitivity to Thermolysin of the two activities in isolated chloroplasts (Figure 5a), suggests that they are both associated with the outer envelope membrane. In Arabidopsis, the main MGDG synthase activity encoded by *MGD1* is associated with the inner envelope membrane facing the intermembrane space, whereas the DGDG synthase, encoded by *DGD1*, is associated with the outer envelope membrane facing the cytosol (Benning and Ohta, 2005). Additional MGDG synthases MGD2 and MGD3 are present in the outer envelope membrane in Arabidopsis, but are thought to be conditionally involved in the synthesis of galactoglycerolipids during phosphate starvation or in specific tissues (Kobayashi *et al.*, 2009). How the products of the two enzymes move between the envelope membranes in Arabidopsis or any other organism is currently unknown.

Galactoglycerolipid metabolism is altered in *tgd2*

A first indication that MGDG synthesis and turnover are affected in the *tgd2* mutant arises from the fact that *tgd2* accumulates TAG with 16:4 and 18:3 acyl groups, typically found only in MGDG (Figure 1d,e). Moreover, osmium tetroxide-stained lipid droplets of *tgd2* (Figure 3d–f) appeared darker compared with those of the PL (Figure 3c), consistent with an increased desaturation of acyl groups associated with lipid droplets (Bahr, 1954; Korn, 1967).

Second, altered MGDG metabolism in the *tgd2* mutant became obvious during acetate pulse-chase labeling studies. While the steady-state bulk levels of MGDG and DGDG in *tgd2* were similar to those of the PL (Figure 1b), acetate-labeling experiments and subsequently direct measurements of MGDG synthase activity in isolated chloroplasts showed that MGDG is more actively synthesized in *tgd2* (Figures 4 and 5a). Interestingly, this higher level of MGDG labeling did not translate into higher or more rapid labeling of DGDG presumably formed by the galactosylation of MGDG. In fact, this result would be consistent with an impairment in the conversion of MGDG into DGDG in the *tgd2* mutant. Similarly, UDP-galactose labeling of isolated chloroplasts showed a decrease in the conversion of MGDG into DGDG in the *tgd2* mutant, as the ratio of labeled DGDG to MGDG strongly decreased (Figure 5b). It should be noted that in this assay DGDG is more highly labeled than MGDG, which is opposite to what is observed with isolated Arabidopsis chloroplasts (Xu *et al.*, 2005). One reason could be that in Chlamydomonas substrate channeling occurs between the MGDG and DGDG synthases, which is decreased in the *tgd2* mutant, indicated by the strongly decreased ratio of labeled DGDG to MGDG. Another reason might be the absence of SFR2 from Chlamydomonas, such that there is no further redistribution of label from MGDG into higher order galactoglycerolipids.

The ways in which TGD2 might be affecting galactoglycerolipid metabolism in Chlamydomonas are outlined in Figure 8. Formally based on the labeling data alone, TGD2 could provide MGDG substrate to the DGDG synthase; however, TGD2 is probably a component of a lipid transporter shuttling lipids between the outer and the inner envelope membranes, whereas the two galactoglycerolipid synthases appear to be both localized in the outer envelope membrane in Chlamydomonas. Because we do not know the lipid substrate of this transporter, it might well be that the TGD1, 2, 3 complex transfers galactoglycerolipids from the outer to the inner envelope membrane. An alternative possibility is that TGD2 as proposed for Arabidopsis is involved in transferring PtdOH from the outer to the inner envelope membrane. After all, it is similar to substrate binding proteins associated with ABC transporters, and binds primarily to PtdOH, just like the TGD2 orthologue from Arabidopsis (Figure 7). Its absence could lead to an increase in PtdOH in the outer envelope membrane. We indeed observed an increase in cellular PtdOH content in the *tgd2* mutant (Figure 1b), although we could not determine the membrane association of this additional PtdOH. As is known for the Arabidopsis MGDG synthase (Dubots *et al.*, 2010), if associated with the outer envelope membrane, this increased PtdOH content could stimulate MGDG synthase activity, leading to increased MGDG biosynthesis, as observed in the *tgd2* mutant (Figure 8). In fact, there is some similarity with the labeling results obtained for Arabidopsis *tgd* mutants (Xu *et al.*, 2003, 2005). First, Arabidopsis *tgd1–1* showed initially a strongly increased incorporation of label into MGDG during acetate pulse-chase labeling (Xu *et al.*, 2003). Second, differences in the labeling of MGDG and DGDG are also increased in the Arabidopsis *tgd1–1* mutant (Xu *et al.*, 2003). Thirdly, during UDP-galactose labeling of isolated chloroplasts,

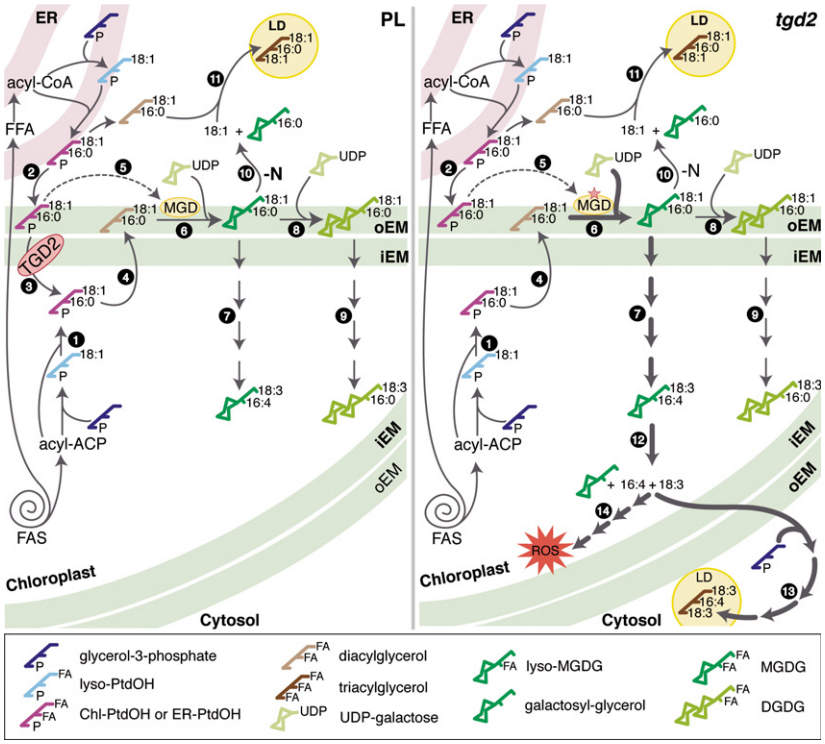

Figure 8. Proposed model of CrTGD2 function.

Different steps (as numbered in solid circles) involved in galactoglycerolipid synthesis are shown in the parental line (PL, left panel) and in the *tgd2* mutant (right panel). Lipid molecular species symbols are explained in a box below the scheme. Fatty acid synthesis (FAS) takes place in the chloroplast generating acyl groups bound to acyl carrier protein (acyl-ACP) used for the synthesis of chloroplast-derived phosphatidic acid (Chl-PtdOH) (1). Free fatty acids (FFA) are also exported to the endoplasmic reticulum (ER) and activated to acyl-CoAs for the synthesis of ER-derived PtdOH (ER-PtdOH), which is then returned to the chloroplast outer envelope membrane (oEM) (2). It is postulated that the two PtdOHs derived from the two different pathways in Chlamydomonas cannot be distinguished, unlike those produced in plants. TGD2 situated in the chloroplast inner envelope membrane (iEM) transports ER-PtdOH from the oEM to the stroma side of the iEM (Loria *et al.*, 1999). PtdOH from both sources can give rise to diacylglycerol (4). On the oEM, PtdOH stimulates MGDG synthase (MGD) (5) to produce MGDG from diacylglycerol and UDP-galactose (6). This newly synthesized MGDG composed of 18:1 and 16:0 acyl chains is a common substrate for three reactions. First, desaturation by MGDG-specific desaturases (7) produces mature MGDG with 18:3 and 16:4 acyl chains. Second, DGDG synthesis (8) yields newly synthesized DGDG with 18:1 and 16:0 acyl chains, which then undergoes desaturation (9), resulting in mature DGDG with mainly 18:3 and 16:0 acyl chains. Third, under N deprivation (Villena *et al.*, 2004), newly synthesized MGDG is degraded (10) by the action of PLASTID GALACTOGLYCEROLIPID DEGRADATION 1 (PGD1). Fatty acids derived from PGD1 degradation are then used for the synthesis of triacylglycerol (11) containing 18:1 and 16:0 acyl chains, which is stored in lipid droplets (LD).

In the *tgd2* mutant lacking TGD2, ER-PtdOH accumulates in the oEM and hyper-stimulates MGDG synthase (5), indicated by the star. This results in higher MGDG synthesis (6), indicated with thick arrows. Note that MGDG in the *tgd2* mutant is primarily synthesized from Chl-PtdOH. Under normal growth conditions, the desaturation of MGDG is more efficient than the degradation by PGD1 or synthesis of DGDG leading to an increased formation of mature MGDG. To avoid an accumulation of mature MGDG it is then degraded by galactolipase(s) (12), yielding 16:4 and 18:3 fatty acids or diacylglycerol with these two acyl groups. These lipid precursors are exported to the cytosol to give rise to triacylglycerol unique to the *tgd2* mutant (13). The additional MGDG molecules produced, or fatty acids derived from them, can also be substrates for lipid peroxidation (14), resulting in the accumulation of reactive oxygen species (ROS), presumably causing the lower viability of the *tgd2* mutant.

MGD1 activity of *tgd1–1* was increased whereas DGDG labeling did not increase (Xu *et al.*, 2005). Thus, the disruption of the TGD complex in both organisms seems to stimulate MGDG synthesis without stimulating DGDG synthesis, and formally could appear as a disruption in the transfer of precursors to the DGDG synthase in labeling experiments.

What happens to MGDG as it is metabolized in the *tgd2* mutant?

It is critical for the cell to maintain a set ratio of the non-bilayer forming lipid, MGDG, and the bilayer forming lipid, DGDG, in its photosynthetic membrane (Dörmann and Benning, 2002). Because MGDG synthesis is increased over that of DGDG in the *tgd2* mutant, to maintain lipid homeostasis and prevent an accumulation of bulk MGDG, its turnover rate must also be increased, as suggested by the acetate pulse-chase labeling experiment (Figure 4). As acyl groups normally specifically found in MGDG of the PL are present in TAG accumulating in the *tgd2* mutant (Figure 1d,e), it appears that some of the DAG moieties of MGDG or its acyl groups are converted to TAG, and are sequestered in lipid droplets (Figure 3d–f). In plants, MGDG can be hydrolyzed, and its DAG or acyl groups are

converted to TAG stored in plastoglobuli inside the plastid during photosynthetic stress (Youssef *et al.*, 2010), or during leaf senescence (Kaup *et al.*, 2002). Thus lipid droplets may serve as a buffer for storing otherwise toxic acyl groups derived from membrane lipids. In addition, TAG synthesis in Chlamydomonas may involve the release of acyl groups from newly formed MGDG by the activity of the lipase PGD1 (Figure 8), as has been shown to occur during N deprivation (Li *et al.*, 2012).

In the case of the *tgd2* mutant of Chlamydomonas, lipid droplets were observed in the cytosol in contact with the outer envelope membrane of the chloroplast (Figure 3g). This observation supports the hypothesis that Chlamydomonas can synthesize TAG in chloroplast membranes (Fan *et al.*, 2011; Liu and Benning, 2013). The Arabidopsis *tgd* mutants, e.g. *tgd1–1*, also accumulate TAG in the cytosol of leaves (Xu *et al.*, 2005); however, the TAG accumulating in the Arabidopsis *tgd1–1* mutant has an acyl profile more similar to that of PtdCho, but not MGDG, as in the case of Chlamydomonas *tgd2.* It was concluded that the accumulation of TAG in the *tgd1–1* mutant was the result of increased conversion of lipid precursors accumulating at the ER because of impaired ER to chloroplast lipid trafficking. TAG accumulation in Arabidopsis *tgd1–1* involves the conversion of PtdCho by phospholipid:DAG acyltransferase (PDAT, Fan *et al.*, 2013). In addition, studies on the Arabidopsis *tgd1–1 sfr2* double mutant revealed that the DAG moiety of TAG accumulating in the Arabidopsis *tgd1–1* mutant is derived from DAG generated by SFR2 activity (Fan *et al.*, 2014). As Chlamydomonas lacks SFR2 activity, however, the mechanism of TAG biosynthesis in the Chlamydomonas *tgd2* mutant must be different.

It also seems likely that acyl groups derived from MGDG undergo a different fate, as they can become oxidized, as seen in the higher level of malondialdehyde derived from fatty-acid peroxidation in the *tgd2* mutant (Figure 2c). It is largely accepted that polyunsaturated fatty acids are targets for oxidation by autooxidation or lipoxygenases (Feussner and Wasternack, 2002). Products of lipid peroxidation are mainly aldehydes, which are toxic to nucleic acids and proteins (Esterbauer *et al.*, 1991). Thus, it seems possible that the increased oxidization of MGDG-derived acyl groups in *tgd2* leads to the lower viability of *tgd2* in prolonged cultures (Figures 2a and 3i).

Does CrTGD2 play a role in the transfer of lipids from the ER to the chloroplast?

In the Arabidopsis *tgd1,2,3,4* mutants, an increase in the ratio of C16/C18 acyl groups of thylakoid lipids indicates a lack of lipid trafficking from the ER to the chloroplast (Xu *et al.*, 2003, 2008; Awai *et al.*, 2006; Lu *et al.*, 2007). In addition, changes in acetate pulse-chase labeling of MGDG in *tgd1–1* seedlings (a lack of a transient decrease in MGDG labeling in the mutant as lipid precursors move from the chloroplast to the ER, and then return) also indicates the lack of lipid transfer between the two compartments (Xu *et al.*, 2003). A similar, albeit more subtle, change in the labeling time course for MGDG was observed for the Chlamydomonas *tgd2* mutant (Figure 4, top panel, Figure S11). Thus these labeling data suggest that lipid precursors could be transferred from the ER to the chloroplast envelope membranes for the synthesis of thylakoid lipids. If this conclusion is correct, the ER-located lyso-PtdOH acyl transferase must have a different substrate specificity in Chlamydomonas compared with Arabidopsis to explain the absence of C18 fatty acids at the *sn–2* position of thylakoid lipids in Chlamydomonas. Thus, a thorough analyses of the acyltransferases in Chlamydomonas will be required to ultimately solve this conundrum.

As in Arabidopsis, subcellular localization and protease protection assays suggest that CrTGD2 is localized in the inner envelope membrane of the chloroplast (Figure 6a,b). Furthermore, similar to AtTGD2 (Awai *et al.*, 2006; Lu and Benning, 2009; Roston *et al.*, 2011), *in vitro* lipid binding assays showed that CrTGD2 binds primarily to PtdOH (Figure 7a,b), which is a candidate for transferred lipid species. Phylogenetic analyses showed that CrTGD2 is in the same clade as plant orthologues, but not bacterial orthologues (Figure S8). However TGD2 proteins from either Arabidopsis or Chlamydomonas were not functional in the opposite host in our hands, respectively (Figures S9 and S10), perhaps because both proteins are too divergent to function in a heterologous complex. Based on all the other data presented here, however, it is likely that the TGD2 protein of Chlamydomonas is also a component of a lipid transporter, transferring lipid precursors between the envelope membranes, as proposed for the homologous system in Arabidopsis. As TGD4 and TGD5 are seemingly absent from Chlamydomonas, however, it remains to be seen what proteins might be involved in lipid transfer between the ER and the outer envelope membrane in Chlamydomonas. Furthermore, because the actual lipid species transported is not yet known, a possibility remains that the TGD1, 2, 3 complex of Chlamydomonas also plays a role in the transfer of the galactoglycerolipids synthesized at the chloroplast outer envelope membrane to the inner envelope membrane in Chlamydomonas.

EXPERIMENTAL PROCEDURES

Algal strains and growth conditions

Chlamydomonas reinhardtii cell wall-less strain dw15.1 (cw15, nit1, mt^+), provided by Arthur Grossman (Carnegie Institute for Science, Department of Plant Biology, Stanford University), was used as wild-type PL with regards to *TGD2* to generate the *tgd2* mutant. A cell-walled strain CC-198 (er-u-37, str-u-2-60, mt^-) obtained from the Chlamydomonas Resource Center (http://chlamycollection.org/) was used to generate *tgd2* cell-walled progenies for linkage analyses and for TEM. Unless specified, the

algal cultures were grown in Tris-acetate-phosphate (TAP) medium (Gorman and Levine, 1965). For all experiments except for chloroplast preparation, algal cultures were grown under continuous light at 80 μmol m^{-2} sec^{-1} and at 22°C. The cell concentration was monitored with a Z2 Coulter Counter (Beckman Coulter, http://www.beckmancoulter.com).

Generation of *tgd2* mutant and genetic analyses

The *tgd2* mutant was generated by insertional mutagenesis in the same experiment as described previously for the *cht7* mutant (Tsai *et al.*, 2014). The details of the genetic analyses are described in Appendix S2. Details about the bacterial artificial chromosomes used for genetic complementation can be found in Table S1. Sequences of primers used for testing genetic complementation are listed in Table S2.

DNA isolation and Southern-blot analyses

DNA isolation was carried out as previously described by Keb-Llanes *et al.* (2002), with some modifications, as detailed in Appendix S2. Southern-blot analyses was performed with the same probe as described by Li *et al.* (2012).

Whole-genome resequencing

The genome of the *tgd2* mutant was sequenced by Illumina Hi-Seq using the paired-end method at the MSU-Research Technology Support Facility. Details of the analyses are described in Appendix S2. The sequences of primers used for identifying the deletion can be found in Table S2.

Lipid analyses

Total lipid was extracted as previously described by Bligh and Dyer (1959), from pellets of either freshly harvested cultures or from pellets stored at −80°C. In general, pellets from 15 ml of algal culture were resuspended in 3 ml of extraction solvent. The extracted lipids were dried under an N_2 stream and stored at −20°C. Individual lipids were separated on thin layer chromatography (TLC) plates (TLC Silica gel 60; EMD Millipore, http://www.emdmillipore.com). For PtdOH separation, TLC plates treated with ammonium sulfate (Benning and Somerville, 1992) were employed. Different solvents were used for different lipid classes: for neutral lipids, petroleum ether, diethyl ether and acetic acid (80 : 20 : 1, v/v); for polar lipids, chloroform, methanol, acetic acid and water (75 : 13 : 9 : 3, v/v); for PtdOH, chloroform, methanol and ammonium hydroxide (65 : 25 : 5, v/v); and for oligogalactolipids, chloroform, methanol, 0.9% sodium chloride and water (60 : 35 : 4 : 4, v/v). Lipids on TLC plates were visualized by briefly staining with iodine vapor. Alternatively, galactoglycerolipids were stained with α–naphthol as described by Wang and Benning (2011). Lipids were isolated and processed for the generation of fatty acid methyl esters (FAMEs), as described by Benning and Somerville (1992). The quantification of FAMEs was performed by gas liquid chromatography using an HP6890 instrument equipped with a DB-23 column (both Agilent Technologies, http://www.agilent.com), with running conditions and temperature profile as described by Zäuner *et al.* (2012).

Viability assay

The PL (dw15.1), *tgd2* mutant and *TGD2 tgd2* complemented line inoculated at 0.5 million cells ml^{-1} were grown in TAP medium. Cells were harvested at day 3, 7, 14, 21 and 28 for viability staining, lipid analyses and thiobarbituric acid-reactive-substances (TBARS) assay. Viability staining was performed as described by Chang *et al.* (2005), with minor modifications. The cell samples were mixed with an equal volume of staining solution (0.0252% methylene blue, 0.0252% phenosafranin and 5% ethanol) and incubated for 5 min. The two dyes are excluded from living cells, which remain green, whereas dead cells take up the dye and are stained purple. The two cell types were counted with a hemocytometer. For lipid analyses, cells were harvested as described above, flash frozen in liquid N_2, and stored at −80°C for later lipid analyses (see above).

Lipid peroxidation was estimated with a TBARS assay. Two aliquots of 5–10 ml of algal culture were harvested by centrifugation as described, and the algal pellets were resuspended in 1 ml of 20% trichloroacetic acid, with or without 0.5% thiobarbituric acid. The mixtures were heated at 95°C for 15 min. Absorbance was measured at 440, 532 and 600 nm. The concentration of malondialdehyde was calculated as described by Hodges *et al.* (1999).

Transmission electron microscopy

Walled strains were fixed as previously described (Harris, 1989). Images were taken with a JEOL100 CXII instrument (Japan Electron Optics Laboratories, http://www.jeol.co.jp).

Phylogenetic analyses

The analyses was performed as detailed under Appendix S2.

Heterologous complementation analyses

The heterologous complementation analyses of the *tgd2* mutant was performed as described in detail in Appendix S2. Sequences of primers used for generating constructs are listed in Table S3.

[^{14}C]Acetate pulse-chase labeling

The different lines were grown in 200 ml of TAP medium to mid-log phase. After 10-fold concentration into 20 ml TAP medium, 10 μl of 1 mCi ml^{-1} [^{14}C]sodium acetate (55 mCi $mmol^{-1}$) was added to the culture. The cultures were incubated at room temperature (22–25°C) for 1–2 h until the incorporation of label reached 20–40%. To initiate the chase, the cultures were centrifuged at 3000 ***g*** for 3 min. The cell pellets were then resuspended in 200 ml of unlabeled TAP medium, and the cultures were incubated at room temperature. At given intervals, 20 ml of the cultures were harvested. Individual lipids were separated on TLC plates as described above. Silica powder containing each lipid was isolated from the TLC plates and subjected to liquid scintillation counting in 10 ml of complete counting cocktail 4a20™ (Research Products International Corp., http://www.rpicorp.com). Radioactivity was measured with a PerkinElmer Liquid Scintillation Analyzer Tri-Carb 2800TR.

DsRED-CrTGD2 pLW01, *DsRED-AtTGD2* pLW01 and *DsRED* pLW01 constructs, recombinant protein expression and purification

Details of the construction of the plasmids and recombinant protein production are as described in Appendix S2. Primers used in this experiment are listed in Table S3.

CrTGD2 antibody

The DsRED-CrTGD2 fusion protein was used as an antigen to raise antiserum in rabbits (Cocalico Biologicals, http://www.cocalicobiologicals.com). The antigen was prepared with Freund's adjuvant

and inoculated in rabbits with three additional boosts. Two test bleeds were checked for immunoreaction against pre-bleed with Chlamydomonas PL and *tgd2* mutant proteins. Final bleed antiserum was used as primary antibody for the detection of immunoreactions.

Immunoblotting

Protein samples for the localization of CrTGD2 and for heterologous *tgd2* complementation analyses were resuspended in protein extraction buffer (0.1 M Tris-HCl, pH 6.8, 1% SDS, 15% glycerol and 5% β–mercaptoethanol). The mixtures were incubated at 95°C for 5 min. The protein was cooled down on ice and centrifuged at 20 000 ***g*** for 10 min at 4°C. Pellets were discarded. Protein concentrations were determined with bovine serum albumin (BSA) as a standard, according to the method described by Bradford (1976). In general, the equivalent of 10 μg of protein (2 μg of chlorophyll for the experiments described in Figure 6b; 40 μg of protein for the experiments described in Figure S9b) were separated by SDS-PAGE. The proteins were then transferred to polyvinylidene difluoride (PVDF) membranes. The membranes were incubated in blocking solution for 30 min (5% non-fat dry milk in TBST buffer containing 20 mM Tris-HCl, pH 7.5, 150 mM NaCl and 0.05% Tween 20, v/v). Following the addition of primary antiserum in blocking solution, the membranes were incubated at 4°C overnight. The membranes were washed six times with TBST at 5–min intervals. Secondary antisera conjugated with horseradish peroxidase were incubated with the membranes for 1–2 h at room temperature. The membranes were washed again as described previously prior to the detection of immunoreaction with Clarity™ Western ECL Substrate (BIO-RAD, http://www.bio-rad.com) as the substrate, and using a ChemiDoc™ MP Imaging System (BIO-RAD). Antibodies against CrTGD2, Tic40 (provided by John Froehlich, Michigan State University), BIP (SC-33757 Santa Cruz Biotechnology, Inc., http://www.scbt.com), cytochrome *c* (BD Pharmingen, http://www.bdbiosciences.com), Toc34 (AS07 238, Agrisera, http://www.agrisera.com), ARC6 (provided by Katherine W. Osteryoung, Michigan State University) and AtTGD2 (Awai *et al.*, 2006) were used at 1 : 500, 1 : 2000, 1 : 1000, 1 : 250, 1 : 10 000, 1 : 2500 and 1 : 2000 dilutions, respectively. Secondary anti-rabbit antibodies were used for each primary antibody, except for anti-cytochrome *c*, for which an anti-mouse antibody (Sigma-Aldrich, http://www.sigmaaldrich.com) was used.

In the case of the lipid binding assay described below, the protein samples were resuspended in 2× SDS sample buffer (0.12 M Tris-HCl, pH 6.8, 4% SDS, 20% glycerol, 10% β–Mercaptoethanol and 0.05% bromophenol blue) and processed as described above. The protein samples were separated by SDS-PAGE and transferred to PVDF membranes. These membranes were processed in the same manner as described above. Primary and secondary antibodies were the His-tag antibody (GenScript, http://www.genscript.com) and anti-mouse conjugated with horseradish peroxidase, respectively. The immunoreaction was detected as described above.

Subcellular fractionation

Chlamydomonas PL dw15.1 was grown under 12–h light and 12–h dark cycles to mid-log phase. A 500-ml culture was harvested by centrifugation at 3000 ***g*** for 10 min at 4°C. Isolation of chloroplast, mitochondrial and microsomal membranes was based on a procedure described in Klein *et al.* (1983), with modifications. In brief, cells were broken by digitonin. The pellet from centrifugation at 800 ***g*** was considered the chloroplast fraction. The chloroplasts were further purified on a 20–40–65% Percoll step gradient made with isotonic solution. Intact chloroplasts were obtained at the transition between 40 and 65% Percoll layers, following centrifugation at 4000 ***g*** for 15 min at 4°C. The supernatant of centrifugation at 800 ***g*** contained mitochondria and microsomal membranes. This supernatant was centrifuged at 5000 ***g*** for 10 min at 4°C. The pellet from this centrifugation contained a mitochondrial crude fraction that was further purified, as previously described in Eriksson *et al.* (1995) using a 20% Percoll gradient made from isotonic solution compatible with the chloroplast isolation buffer. The supernatant from the 5000 ***g*** centrifugation was further centrifuged at 100 000 ***g*** for 90 min at 4°C. The pellet from this centrifugation was considered the microsomal membrane fraction. All fractions were processed by immunoblotting as described above.

Protease protection assay

Isolated chloroplasts were treated with Thermolysin or Trypsin. For Thermolysin treatment, 50 μg ml^{-1} chlorophyll equivalents were incubated with 0–200 μg ml^{-1} Thermolysin in buffer containing 20 mM Tricine-NaOH, pH 7.7, 150 mM mannitol, 1 mM $MgCl_2$, 1 mM $MnCl_2$, 2 mM EDTA and 0.5 mM $CaCl_2$. The treatment was carried out on ice for 15 min. The reaction was stopped with the above buffer by adding 10 mM EDTA. The treated chloroplasts were overlaid on a 40% Percoll gradient made from treatment buffer with the addition of 5 mM EDTA. The chloroplasts were centrifuged at 1500 ***g*** for 5 min. The pellet was washed with treatment buffer containing 5 mM EDTA. Trypsin treatment was carried out in a similar manner with a few modifications. The Trypsin treatment buffer was the same as the Thermolysin buffer without 0.5 mM $CaCl_2$. The reaction was stopped with buffer containing 200 μg ml^{-1} Trypsin inhibitor. Instead of 5 mM EDTA in the 40% Percoll gradient and in the wash buffer, 100 μg ml^{-1} Trypsin inhibitor was added. Protease-treated chloroplasts were processed for immunoblotting as described above, or were assayed for MGDG synthase activity.

MGDG synthase assay

Intact chloroplasts either treated with 100 μg ml^{-1} Thermolysin or left untreated, as described above, were resuspended at 125 μg chlorophyll equivalent in 100 μl of assay buffer containing 20 mM Tricine-NaOH, pH 7.7, 150 mM mannitol, 5 mM $MgCl_2$ and 2.5 mM EDTA. The reaction was started by adding 0.3 μCi of UDP-[^{14}C] galactose (300 mCi $mmol^{-1}$), and then incubated at room temperature under light for 2 min. Lipid was extracted as a means to stop the reaction. MGDG and DGDG were separated by TLC, and radioactive lipids were analyzed as described above.

Lipid binding assay

Liposomes consisting of different test lipids were prepared with dioleoyl PtdCho at a 40 : 60% molar ratio. The mixtures of tested lipid and PtdCho were dried under a stream of N_2. Dried lipids were resuspended in 200 μl of TBS (50 mM Tris-HCl, pH 7.0, and 0.1 M NaCl). The mixtures were incubated in a water bath at the highest lipid transition temperature (37°C for dioleoyl lipids) for 1 h. The liposomes were washed once and resuspended in 95 μl of TBS; 5 μl of 3.7 μg DsRED-AtTGD2-6xHis and 2 μg of DsRED, or 3.6 μg of DsRED-CrTGD2-6xHis and 2 μg DsRED were added to the liposomes. DsRED served as an internal negative control. The mixtures were incubated at room temperature for 30 min. Liposome–protein complexes were recovered by centrifugation at 13 000 ***g*** for 10 min at 4°C. The pellets were washed twice in TBS. The liposome–protein pellets were processed to detect the DsRED proteins by immunoblotting, as described above.

Accession numbers

Read sequences of the *tgd2* mutant obtained from whole-genome resequencing can be found in the Sequence Read Archive of the National Center for Biotechnology Information under accession number SRP061379. Chlamydomonas TGD2 sequence accession number Cre16.g694400.t1.2 was obtained from the Joint Genome Institute. Arabidopsis TGD2 sequence accession number AT3G20320 was obtained from The Arabidopsis Information Resource (http://www.arabidopsis.org). The accession numbers used for the phylogenetic tree reconstruction are shown in Figure S8, following the species names.

ACKNOWLEDGEMENTS

We are grateful to Dr Simone Zäuner and Dr Yang Yang for valuable discussions. We would like to thank Dr Likit Preeyanon for helping with *de novo* genome assembly and Alicia Pastor for helping with electron microscopy. We thank Tomomi Takeuchi and Dr Shin-Han Shiu for helping with the construction of the phylogenetic tree. We thank Dr Setsuko Wakao and Dr John Froehlich for valuable suggestions for subcellular fractionation and the protease protection assay, respectively. We appreciate Dr Pawin Ittisamai for taking photographs in Figure 2a. JW has been supported by a Royal Thai Government Scholarship. This work was supported in part by grants to CB from the US NSF (MCB 1157231), the US AFOSR (FA9550-11-1–0264), by a Strategic Partnership grant from the MSU Foundation, and by MSU AgBioResearch.

SUPPORTING INFORMATION

Additional Supporting Information may be found in the online version of this article.

Figure S1. Separation of phosphatidic acid (PtdOH) and oligogalactoglycerolipids by thin-layer chromatography (TLC).

Figure S2. Cell viability and acyl group composition of TAGs during extended culturing time.

Figure S3. Ultrastructure of chloroplast membranes.

Figure S4. Southern-blot analysis of the *tgd2* mutant and the PL (dw15.1).

Figure S5. Analyses of progenies from crosses between *tgd2* and CC-198.

Figure S6. Mutant locus in the *tgd2* genome and complementation.

Figure S7. Amino acid sequence alignment of AtTGD2 and CrTGD2.

Figure S8. Phylogenetic analyses of CrTGD2 homologues.

Figure S9. Lack of Arabidopsis TGD2 complementation in the Chlamydomonas *tgd2* mutant.

Figure S10. Lack of Chlamydomonas TGD2 complementation in the Arabidopsis *tgd2* mutant.

Figure S11. Pulse-chase [^{14}C]acetate labeling of MGDG in the PL (dw15.1).

Table S1. Bacterial artificial chromosomes (BACs) used in the *tgd2* complementation analyses.

Table S2. Sequences of primers for probing the deletion in chromosome 16 in the *tgd2* mutant.

Table S3. Sequences of primers used for constructing plasmids as indicated.

Appendix S1. Amino acid sequence alignment of Mammalian Cell Entry domains of CrTGD2 homologues used for building the phylogenetic tree in Figure S8.

Appendix S2. Supporting Materials and Methods.

REFERENCES

Awai, K., Marechal, E., Block, M.A., Brun, D., Masuda, T., Shimada, H., Takamiya, K., Ohta, H. and Joyard, J. (2001) Two types of MGDG synthase genes, found widely in both 16:3 and 18:3 plants, differentially mediate galactolipid syntheses in photosynthetic and nonphotosynthetic tissues in *Arabidopsis thaliana*. *Proc. Natl Acad. Sci. USA*, **98**, 10960–10965.

Awai, K., Xu, C., Tamot, B. and Benning, C. (2006) A phosphatidic acid-binding protein of the chloroplast inner envelope membrane involved in lipid trafficking. *Proc. Natl Acad. Sci. USA*, **103**, 10817–10822.

Bahr, G.F. (1954) Osmium tetroxide and ruthenium tetroxide and their reactions with biologically important substances: electron stains III. *Exp. Cell Res.* **7**, 457–479.

Benning, C. (2009) Mechanisms of lipid transport involved in organelle biogenesis in plant cells. *Annu. Rev. Cell Dev. Biol.* **25**, 71–91.

Benning, C. and Ohta, H. (2005) Three enzyme systems for galactoglycerolipid biosynthesis are coordinately regulated in plants. *J. Biol. Chem.* **280**, 2397–2400.

Benning, C. and Somerville, C. (1992) Isolation and genetic complementation of a sulfolipid-deficient mutant of *Rhodobacter sphaeroides*. *J. Bacteriol.* **174**, 2352–2360.

Bligh, E.G. and Dyer, W.J. (1959) A rapid method of total lipid extraction and purification. *Can. J. Biochem. Physiol.* **37**, 911–917.

Boudière, L., Michaud, M., Petroutsos, D. *et al.* (2014) Glycerolipids in photosynthesis: composition, synthesis and trafficking. *Biochim. Biophys. Acta*, **1837**, 470–480.

Bradford, M.M. (1976) A rapid and sensitive method for the quantitation of microgram quantities of protein utilizing the principle of protein-dye binding. *Anal. Biochem.* **72**, 248–254.

Casali, N. and Riley, L.W. (2007) A phylogenomic analysis of the Actinomycetales mce operons. *BMC Genom.* **8**, 60.

Chang, C.W., Moseley, J.L., Wykoff, D. and Grossman, A.R. (2005) The LPB1 gene is important for acclimation of *Chlamydomonas reinhardtii* to phosphorus and sulfur deprivation. *Plant Physiol.* **138**, 319–329.

Cline, K., Werner-Washburne, M., Andrews, J. and Keegstra, K. (1984) Thermolysin is a suitable protease for probing the surface of intact pea chloroplasts. *Plant Physiol.* **75**, 675–678.

Dörmann, P. and Benning, C. (2002) Galactolipids rule in seed plants. *Trends Plant Sci.* **7**, 112–118.

Dubots, E., Audry, M., Yamaryo, Y., Bastien, O., Ohta, H., Breton, C., Marechal, E. and Block, M.A. (2010) Activation of the chloroplast monogalactosyldiacylglycerol synthase MGD1 by phosphatidic acid and phosphatidylglycerol. *J. Biol. Chem.* **285**, 6003–6011.

Eriksson, M., Gardestrom, P. and Samuelsson, G. (1995) Isolation, purification, and characterization of mitochondria from *Chlamydomonas reinhardtii*. *Plant Physiol.* **107**, 479–483.

Esterbauer, H., Schaur, R.J. and Zollner, H. (1991) Chemistry and biochemistry of 4-hydroxynonenal, malonaldehyde and related aldehydes. *Free Radic. Biol. Med.* **11**, 81–128.

Fan, J., Andre, C. and Xu, C. (2011) A chloroplast pathway for the de novo biosynthesis of triacylglycerol in *Chlamydomonas reinhardtii*. *FEBS Lett.* **585**, 1985–1991.

Fan, J., Yan, C. and Xu, C. (2013) Phospholipid: diacylglycerol acyltransferase-mediated triacylglycerol biosynthesis is crucial for protection against fatty acid-induced cell death in growing tissues of Arabidopsis. *Plant J.* **76**, 930–942.

Fan, J., Yan, C., Roston, R., Shanklin, J. and Xu, C. (2014) Arabidopsis lipins, PDAT1 acyltransferase, and SDP1 triacylglycerol lipase synergistically direct fatty acids toward β-oxidation, thereby maintaining membrane lipid homeostasis. *Plant Cell*, **26**, 4119–4134.

Fan, J., Zhai, Z., Yan, C. and Xu, C. (2015) Arabidopsis TRIGALACTOSYLDIACYLGLYCEROL5 Interacts with TGD1, TGD2, and TGD4 to Facilitate Lipid Transfer from the Endoplasmic Reticulum to Plastids. *Plant Cell*, doi:10.1105/tpc.15.00394 [Epub ahead of print].

Feussner, I. and Wasternack, C. (2002) The lipoxygenase pathway. *Annu. Rev. Plant Biol.* **53**, 275–297.

Frentzen, M., Heinz, E., McKeon, T.A. and Stumpf, P.K. (1983) Specificities and selectivities of glycerol-3-phosphate acyltransferase and monoacylglycerol-3-phosphate acyltransferase from pea and spinach chloroplasts. *Eur. J. Biochem.* **129**, 629–636.

Giroud, C. and Eichenberger, W. (1988) Fatty acids of *Chlamydomonas reinhardtii* – structure, positional distribution and biosynthesis. *Biol. Chem.* **369**, 18–19.

Gorman, D.S. and Levine, R.P. (1965) Cytochrome *f* and plastocyanin: their sequence in the photosynthetic electron transport chain of *Chlamydomonas reinhardtii*. *Proc. Natl Acad. Sci. USA*, **54**, 1665–1669.

Gross, L.A., Baird, G.S., Hoffman, R.C., Baldridge, K.K. and Tsien, R.Y. (2000) The structure of the chromophore within DsRed, a red fluorescent protein from coral. *Proc. Natl Acad. Sci. USA*, **97**, 11990–11995.

Harris, E.H. (1989) *The Chlamydomonas Sourcebook: A Comprehensive Guide to Biology and Laboratory use*. San Diego: Academic Press.

Heinz, E. and Roughan, P.G. (1983) Similarities and differences in lipid metabolism of chloroplasts isolated from 18:3 and 16:3 plants. *Plant Physiol.* **72**, 273–279.

Hodges, D.M., DeLong, J.M., Forney, C.F. and Prange, R.K. (1999) Improving the thiobarbituric acid-reactive-substances assay for estimating lipid peroxidation in plant tissues containing anthocyanin and other interfering compounds. *Planta*, **207**, 604–611.

Hurlock, A.K., Roston, R.L., Wang, K. and Benning, C. (2014) Lipid trafficking in plant cells. *Traffic*, **15**, 915–932.

Jardillier, L., Zubkov, M.V., Pearman, J. and Scanlan, D.J. (2010) Significant CO_2 fixation by small prymnesiophytes in the subtropical and tropical northeast Atlantic Ocean. *ISME J.* **4**, 1180–1192.

Jarvis, P., Dormann, P., Peto, C.A., Lutes, J., Benning, C. and Chory, J. (2000) Galactolipid deficiency and abnormal chloroplast development in the Arabidopsis MGD synthase 1 mutant. *Proc. Natl Acad. Sci. USA*, **97**, 8175–8179.

Kaup, M.T., Froese, C.D. and Thompson, J.E. (2002) A role for diacylglycerol acyltransferase during leaf senescence. *Plant Physiol.* **129**, 1616–1626.

Keb-Llanes, M., González, G., Chi-Manzanero, B. and Infante, D. (2002) A rapid and simple method for small-scale DNA extraction in Agavaceae and other tropical plants. *Plant Mol. Biol. Rep.* **20**, 299.

Kieboom, J., Dennis, J.J., de Bont, J.A.M. and Zylstra, G.J. (1998a) Identification and molecular characterization of an efflux pump involved in *Pseudomonas putida* S12 solvent tolerance. *J. Biol. Chem.* **273**, 85–91.

Kieboom, J., Dennis, J.J., Zylstra, G.J. and de Bont, J.A.M. (1998b) Active efflux of organic solvents by *Pseudomonas putida* S12 is induced by solvents. *J. Bacteriol.* **180**, 6769–6772.

Kim, K., Lee, S., Lee, K. and Lim, D. (1998) Isolation and characterization of toluene-sensitive mutants from the toluene-resistant bacterium Pseudomonas putida GM73. *J. Bacteriol.* **180**, 3692–3696.

Kim, H.U., Li, Y. and Huang, A.H.C. (2005) Ubiquitous and endoplasmic reticulum–located lysophosphatidyl acyltransferase, LPAT2, is essential for female but not male gametophyte development in Arabidopsis. *Plant Cell*, **17**, 1073–1089.

Klein, U., Chen, C., Gibbs, M. and Platt-Aloia, K.A. (1983) Cellular fractionation of *Chlamydomonas reinhardii* with emphasis on the isolation of the chloroplast. *Plant Physiol.* **72**, 481–487.

Kobayashi, K., Awai, K., Nakamura, M., Nagatani, A., Masuda, T. and Ohta, H. (2009) Type-B monogalactosyldiacylglycerol synthases are involved in phosphate starvation-induced lipid remodeling, and are crucial for low-phosphate adaptation. *Plant J.* **57**, 322–331.

Korn, E.D. (1967) A chromatographic and spectrophotometric study of the products of the reaction of osmium tetroxide with unsaturated lipids. *J. Cell Biol.* **34**, 627–638.

Krogh, A., Larsson, B., Von Heijne, G. and Sonnhammer, E.L. (2001) Predicting transmembrane protein topology with a hidden Markov model: application to complete genomes. *J. Mol. Biol.* **305**, 567–580.

Kunst, L., Browse, J. and Somerville, C. (1988) Altered regulation of lipid biosynthesis in a mutant of Arabidopsis deficient in chloroplast glycerol-3-phosphate acyltransferase activity. *Proc. Natl Acad. Sci. USA*, **85**, 4143–4147.

Li, X., Moellering, E.R., Liu, B., Johnny, C., Fedewa, M., Sears, B.B., Kuo, M.-H. and Benning, C. (2012) A galactoglycerolipid lipase Is required for triacylglycerol accumulation and survival following nitrogen deprivation in *Chlamydomonas reinhardtii*. *Plant Cell*, **24**, 4670–4686.

Liu, B. and Benning, C. (2013) Lipid metabolism in microalgae distinguishes itself. *Curr. Opin. Biotech.* **24**, 300–309.

Loria, J.P., Rance, M. and Palmer, A.G. 3rd (1999) A TROSY CPMG sequence for characterizing chemical exchange in large proteins. *J. Biomol. NMR*, **15**, 151–155.

Lu, B. and Benning, C. (2009) A 25-amino acid sequence of the Arabidopsis TGD2 protein is sufficient for specific binding of phosphatidic acid. *J. Biol. Chem.* **284**, 17420–17427.

Lu, B., Xu, C., Awai, K., Jones, A.D. and Benning, C. (2007) A small ATPase protein of Arabidopsis, TGD3, involved in chloroplast lipid import. *J. Biol. Chem.* **282**, 35945–35953.

Malinverni, J.C. and Silhavy, T.J. (2009) An ABC transport system that maintains lipid asymmetry in the Gram-negative outer membrane. *Proc. Natl Acad. Sci. USA*, **106**, 8009–8014.

Melis, A. (2009) Solar energy conversion efficiencies in photosynthesis: minimizing the chlorophyll antennae to maximize efficiency. *Plant Sci.* **177**, 272–280.

Merchant, S.S., Prochnik, S.E., Vallon, O. *et al.* (2007) The Chlamydomonas genome reveals the evolution of key animal and plant functions. *Science*, **318**, 245–250.

Ramos, J.L., Duque, E., Godoy, P. and Segura, A. (1998) Efflux pumps involved in toluene tolerance in *Pseudomonas putida* DOT-T1E. *J. Bacteriol.* **180**, 3323–3329.

Roston, R., Gao, J., Xu, C. and Benning, C. (2011) Arabidopsis chloroplast lipid transport protein TGD2 disrupts membranes and is part of a large complex. *Plant J.* **66**, 759–769.

Roston, R.L., Gao, J., Murcha, M.W., Whelan, J. and Benning, C. (2012) TGD1, -2, and -3 proteins involved in lipid trafficking form ATP-binding cassette (ABC) transporter with multiple substrate-binding proteins. *J. Biol. Chem.* **287**, 21406–21415.

Roughan, P.G. and Slack, C.R. (1982) Cellular organization of glycerolipid metabolism. *Annu. Rev. Plant Physiol.* **33**, 97–132.

Tardif, M., Atteia, A., Specht, M. *et al.* (2012) PredAlgo: a new subcellular localization prediction tool dedicated to green algae. *Mol. Biol. Evol.* **29**, 3625–3639.

Tsai, C.-H., Warakanont, J., Takeuchi, T., Sears, B.B., Moellering, E.R. and Benning, C. (2014) The protein Compromised Hydrolysis of Triacylglycerols 7 (CHT7) acts as a repressor of cellular quiescence in Chlamydomonas. *Proc. Natl Acad. Sci. USA*, **111**, 15833–15838.

Villena, J.A., Roy, S., Sarkadi-Nagy, E., Kim, K.H. and Sul, H.S. (2004) Desnutrin, an adipocyte gene encoding a novel patatin domain-containing protein, is induced by fasting and glucocorticoids: ectopic expression of desnutrin increases triglyceride hydrolysis. *J. Biol. Chem.* **279**, 47066–47075.

Wang, Z. and Benning, C. (2011) *Arabidopsis thaliana* polar glycerolipid profiling by thin layer chromatography (TLC) coupled with gas-liquid chromatography (GLC). *J. Vis. Exp.* **49**, e2518–e2523.

Wang, Z., Xu, C. and Benning, C. (2012) TGD4 involved in endoplasmic reticulum-to-chloroplast lipid trafficking is a phosphatidic acid binding protein. *Plant J.* **70**, 614–623.

Weyer, K., Bush, D., Darzins, A. and Willson, B. (2010) Theoretical maximum algal oil production. *Bioenergy Res.* **3**, 204–213.

Xu, C., Fan, J., Riekhof, W., Froehlich, J.E. and Benning, C. (2003) A permease-like protein involved in ER to thylakoid lipid transfer in Arabidopsis. *EMBO J.* **22**, 2370–2379.

Xu, C., Fan, J., Froehlich, J.E., Awai, K. and Benning, C. (2005) Mutation of the TGD1 chloroplast envelope protein affects phosphatidate metabolism in Arabidopsis. *Plant Cell*, **17**, 3094–3110.

Xu, C., Fan, J., Cornish, A.J. and Benning, C. (2008) Lipid trafficking between the endoplasmic reticulum and the plastid in Arabidopsis requires the extraplastidic TGD4 protein. *Plant Cell*, **20**, 2190–2204.

Youssef, A., Laizet, Y.h., Block, M.A., Maréchal, E., Alcaraz, J.-P., Larson, T.R., Pontier, D., Gaffé, J. and Kuntz, M. (2010) Plant lipid-associated fibrillin proteins condition jasmonate production under photosynthetic stress. *Plant J.* **61**, 436–445.

Zäuner, S., Jochum, W., Bigorowski, T. and Benning, C. (2012) A Cytochrome b5-containing plastid-located fatty acid desaturase from *Chlamydomonas reinhardtii*. *Euk Cell*, **11**, 856–863.

Zerbino, D.R. and Birney, E. (2008) Velvet: algorithms for *de novo* short read assembly using de Bruijn graphs. *Genome Res.* **18**, 821–829.